

Evaluation of Mixing Energy in Laboratory Flasks Used for Dispersant Effectiveness Testing

Vikram J. Kaku¹; Michel C. Boufadel, M.ASCE²; and Albert D. Venosa³

Abstract: The evaluation of dispersant effectiveness used for oil spills is commonly done using tests conducted in laboratory flasks. The success of a test relies on replication of the conditions at sea. We used a hot wire anemometer to characterize the turbulence characteristics in the swirling flask (SF) and the baffled flask (BF), the latter is being considered by the Environmental Protection Agency to replace the prior. We used the measurements to compute the velocity gradient, G and the energy dissipation rate per unit mass, ϵ . The study shows that the mixing in the BF is more uniformly distributed than that in the SF. Flask average energy dissipation rates in the SF were about 2 orders of magnitude smaller than those in the BF. The sizes of the microscales in the BF were found to be much smaller than that in the SF. Also, in the BF, the sizes of the microscales approached the size of oil droplets observed at sea (50–400 μm), which means that the turbulence in the BF closely resembles the turbulence occurring at sea during breaking waves. Hence, the BF is preferable for dispersant testing in the laboratory.

DOI: 10.1061/(ASCE)0733-9372(2006)132:1(93)

CE Database subject headings: Oil spills; Turbulence; Anemometers; Energy dissipation; Velocity; Time series analysis; Data collection.

Introduction

The adverse economic and environmental effects of offshore oil spills are greatest when the oil slick reaches the shoreline. For this reason, much effort is put on preventing offshore oil spills from reaching the shoreline. In calm seas, use of skimmers and booms to collect the oil at sea is the conventional method of cleanup and recovery. In situ burning is also used in such a situation, but it has its limitations. In rough seas, skimming or burning the oil is not effective, and the use of chemical dispersants appears to be the promising approach for cleanup (Naess 1979; Delvigne et al. 1987; NRC 1989; Fingas 2000).

A dispersant is a mixture of surfactants and solvents that causes the oil slick to break into small droplets in a process known as dispersion. (The term “dispersion” used here is from the oil literature and is different from the spreading of chemicals due to the spatial variation of velocity.) The generated small oil droplets get transported or transferred into the water column due to wave action and sea turbulence. They subsequently move away from the contaminated area due to prevailing currents. They

could eventually adhere to suspended particulate matter and/or biodegrade.

Dispersion of oil droplets is enhanced by turbulence due to the mixing energy imposed by waves, especially breaking waves (Delvigne 1993). This means that the artificial dispersion of oil is a chemico-physical process that depends both on the type of dispersant/oil pair and on the sea state. Typically, light and heavy oils are not easily dispersible. In the case of light oils, the formed droplets have to be very small to overcome buoyancy. Hence, a high dosage of dispersant is required to cause the formation of such small droplets. Heavy oils are much more resistant to dispersion because their high viscosity prevents the dispersant from penetrating them, which is a necessary condition to produce dispersed oil droplets. The use of dispersants in very calm or very rough sea is not effective. In very calm seas, the applied dispersant tends to run off the oil and gathers in small pools within the slick. The use of dispersants in very rough seas might not be needed because a high degree of dispersion occurs naturally due to the high energy at sea.

Various field studies and laboratory experiments have been conducted to evaluate the effectiveness of dispersants under various sea conditions. Field studies are accompanied by large experimental uncertainties in the sea; replicates are usually difficult to achieve due to constantly changing climatic conditions and for economic reasons. Hence, smaller scale testing is extensively used to study dispersant effectiveness. Fingas (1991) reports that there are about 50 different laboratory test methods available for determining the effectiveness of dispersants on oil. Examples of commonly used tests include the Swirling flask (SF) test method (Fingas et al. 1987b, 1991; Clayton et al. 1993; Fingas 2000), the Warren Spring Laboratory test method (Byford and Green 1984; Martinelli 1984; Lunel 1993; Lunel and Davies 1996; Fingas 2000), and the Exxon dispersant effectiveness test method (Nordvik et al. 1993; Fiocco et al. 1999; Canevari et al. 2001).

The SF [Fig. 1(a)] test consists of placing a mixture of oil,

¹Research Assistant, Dept. of Mechanical Engineering, Temple Univ., 1947 N. 12th St., Philadelphia, PA 19122.

²Assistant Professor, Dept. of Civil & Environmental Engineering, Temple Univ., 1947 N. 12th St., Philadelphia, PA 19122 (corresponding author). E-mail: boufadel@temple.edu

³Program Manager, Oil Spill Research Program, U.S. Environmental Protection Agency, National Risk Management Research Laboratory, 26 W. Martin Luther King Dr., Cincinnati, OH 45268.

Note. Discussion open until June 1, 2006. Separate discussions must be submitted for individual papers. To extend the closing date by one month, a written request must be filed with the ASCE Managing Editor. The manuscript for this paper was submitted for review and possible publication on November 18, 2003; approved on April 11, 2005. This paper is part of the *Journal of Environmental Engineering*, Vol. 132, No. 1, January 1, 2006. ©ASCE, ISSN 0733-9372/2006/1-93-101/\$25.00.

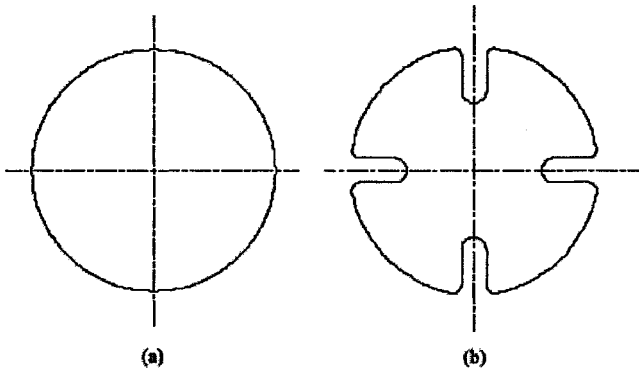


Fig. 1. Schematic cross section of: (a) swirling flask and (b) baffled flask

seawater, and a dispersant in the SF positioned on an orbital (circular motion) shaker (Fingas et al. 1987a, 1997; Clayton et al. 1993; Fingas 2000) then mixing the contents for a specified amount of time, allowing a short settling time, and then extracting the contents from the SF and measuring the concentration of oil dispersed in the water. The claimed advantages of this test are its ease of use and simplicity. Experiments with the SF test have come under scrutiny by the U.S. Environmental Protection Agency (EPA), because of the lack of reproducibility in the hands of different analysts (Venosa et al. 2002), and because it was suspected that the mixing does not resemble the mixing occurring at sea, especially due to breaking waves. The EPA will soon be adopting a new flask, the baffled flask (BF), which has four baffles in it [Fig. 1(b)]. The irregular geometry of the BF results in an apparent over-and-under motion of water flow somewhat more characteristic of the type of mixing that occurs from breaking waves at sea.

As dispersion of oil into fine oil droplets takes place at the smaller scale (i.e., below the 1 cm scale), simulation of these interactions in laboratory experiments is possible because the smallest eddies in the flask are similar to those at sea. This means that, following the work of Delvigne et al. (1987), the energy dissipation rate per unit mass, ε , can be used as an appropriate scaling parameter. The units of ε are watts/kilogram, which is equal to $\text{meter}^2/\text{second}^3$.

The dissipation of kinetic energy occurs due to laminar and turbulent shears within the water. The shear is directly proportional to velocity gradients, which play an important role in the mixing of chemicals, such as oil and dispersant. A well known relation exists between ε and the absolute velocity gradient G (s^{-1}) at every location in the fluid (Camp and Stein 1943; Tennekes and Lumley 1972; Anderson et al. 1984)

$$\varepsilon = \nu G^2 \quad (1)$$

where ν =kinematic viscosity of water ($10^{-6} \text{ m}^2/\text{s}$ at 20°C).

Hence, knowledge of ε is equivalent to knowledge of velocity gradient, and subsequently the intensity of mixing of chemicals. Alternatively, one may use velocity measurements in a selected water body to compute the velocity gradient, and subsequently the energy dissipation rate. This is the approach that we adopt in this work to evaluate energy dissipation rates in the SF and the BF. We used a hot-wire anemometer (HWA) to measure the instantaneous water velocity distributions in the flasks.

Theory

In turbulent mixing, large eddies carry the energy obtained from the general motion of the fluid (Batchelor 1970; Hinze 1987; Frost 1977; Patterson and Zipp 1991). These eddies break into smaller eddies, which in turn break into smaller eddies down to a scale where molecular viscosity effects become dominant. As hypothesized by Kolmogorov (1962), there is a cascade of kinetic energy from the large eddies to smaller ones down to the so-called Kolmogorov scale (less than 1 mm in this work) where the kinetic energy is dissipated by viscous forces due to friction of water molecules on each other.

The small-scale structure of turbulence tends to be independent of any orientation effects, and is thus locally isotropic. In isotropic turbulence, the dissipation rate per unit mass is simplified to (Tennekes and Lumley 1972, p. 66)

$$\varepsilon = 15\nu \overline{\left(\frac{\partial u_i}{\partial x_i}\right)^2} \quad (2)$$

where u_i ($i=x, y, z$)=instantaneous velocity in any “ i ” direction. The mixing due to turbulence is much larger than that due to the spatial variation of the velocity. For this reason, only the turbulence contribution is considered in the evaluation of ε (Rao and Brodkey 1972; Wu and Patterson 1989; Kaku et al. 2002). Considering the orbital motion of the flask, one may write

$$u_i(s, t) = [\overline{U}_i(s) + \tilde{u}_i(s, t)] + u'_i(s, t) \quad (3)$$

$i = x, y, z$

where \overline{U}_i =time-averaged (mean) velocity that depends solely on location; \tilde{u}_i =oscillatory component due to the oscillatory motion of the flask (it depends on both location in the flask and time); and u'_i =component due to turbulence. The oscillatory component could be obtained as a moving average of the time series of u_i (essentially a smooth line that would exist even in the absence of turbulence).

The evaluation of ε in this work will be done using the autocorrelation function approach. The energy dissipation rate per unit mass may be written as (Wu and Patterson 1989; Kresta and Wood 1993)

$$\varepsilon = A \frac{(u'_{\text{rms}})^2}{\tau_{E_i}} \quad (4)$$

where u'_{rms} =root mean square (RMS) value of the turbulent component of velocity, A =constant of order unity; and τ_{E_i} =integral time scale obtained by

$$\tau_{E_i} = \int_0^\infty R_{E_i} dt \quad (5)$$

where R_{E_i} =temporal autocorrelation function, viz.

$$R_{E_i} = \frac{\overline{u'_i(t)u'_i(t+\tau)}}{(u'_i)^2} \quad (6)$$

where τ =time lag. Note that R_{E_i} is assumed to be the same in all directions, a direct consequence of the isotropic turbulence assumption. In practice an upper limit of ∞ is impractical in Eq. (5), so the point of first zero crossing may be used (Wu et al. 1989) (Fig. 3).

The Kolmogorov scale, η , provides an estimate of the smallest eddy that can exist prior to the dissipation by (molecular) viscous friction. It is estimated based on dimensional arguments (Tennekes and Lumley 1972, p. 67) as

$$\eta = \left(\frac{\nu^3}{\varepsilon} \right)^{1/4} \quad (7)$$

The velocity gradient is estimated by rewriting Eq. (1)

$$G = \left(\frac{\varepsilon}{\nu} \right)^{1/2} \quad (8)$$

The above equation of G represents a local velocity gradient, since ε is estimated as a function of position. The flask average velocity gradient, \bar{G} is obtained by taking average of local G values.

Not all turbulent flows manifest churning and foaming. Hence, a quantitative means to detect the presence of turbulence is through evaluation of the Fourier spectrum, which represents the kinetic energy content at various scales. The spectrum in turbulent flows has the following property (Kolmogorov 1941):

$$E \propto k^{-5/3} \quad (9)$$

where k =wave number (inverse of length). For a time series of measurements at a point, a turbulent flow has the following spectrum:

$$E \propto f^{-5/3} \quad (10)$$

where f represents the frequency of velocity fluctuations. Eq. (10) is valid in situations where Taylor's "frozen turbulence" hypothesis is applicable (Monin and Yaglom 1975, p. 11; Hinze 1987, p. 41). The hypothesis stipulates that turbulent eddies are advected without a change in their statistical properties, allowing one therefore to infer these properties from a time series at a point.

Experimental Setup

The experimental setup consisted of a 150 mL SF [Fig. 1(a)], a 200 mL baffled trypsinizing flask, BF [Fig. 1(b)], and an orbital shaker (3518, Lab-Line Instruments Inc.). Each flask contained 120 mL of tap water as the working fluid. The flasks were held in place on the orbital shaker using flask holders. Two rotation speeds of the orbital shaker were considered: 150 and 200 rpm. The diameter of the circle traced by the shaker was 1.9 cm. During rotation, the location of the flasks was measured using a position transducer (PN150-0121, SpaceAge Control Inc.). A HWA (TSI 1210-20W, with single cylindrical sensor) was mounted on the orbital shaker to measure the water speed in the flasks. All measurements were interfaced to a computer using a data-acquisition board (DAS 1401), by Keithley Instruments, Inc. (Cleveland, Ohio) with a built-in analog-to-digital circuit. The data logging software *LABTECH Notebook Pro* (Laboratory Technologies, Inc.) was used.

The radial and tangential (i.e., azimuthal) velocities were measured using the HWA. The HWA is essentially an electric resistor that cools upon passage of water flow. The change in temperature alters the voltage that passes through the resistor. Hence, voltage reading across the HWA provides a surrogate measure of the water velocity. The HWA was calibrated in the velocity range (0–50 cm/s) (see Appendix). The output voltage from HWA at

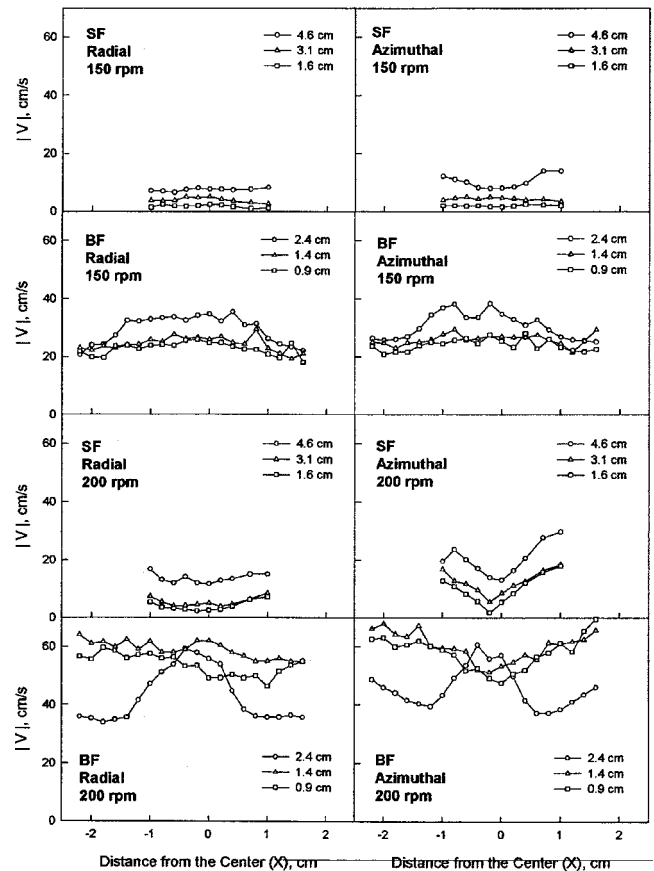


Fig. 2. Magnitude of average radial and azimuthal velocities, $|V|$, at various elevations in swirling flask and baffled flask for 150 and 200 rpm

zero velocities fluctuated from 2.8 to 2.85 V throughout the duration of the experiments. Hence, the uncertainty in measurements is expected to be less than $\pm 4\%$.

The velocities were measured in the center vertical plane of both the flasks at a spatial interval of 2 mm in the horizontal (i.e., radial) direction and 5 mm in the vertical direction. This totaled in 70 locations in the SF and 80 locations in the BF. The data collection frequency was 1,000 Hz, but the response of the whole setup was estimated at about 400 Hz, as noted from the spectrum in Fig. 4(b) where noise was present at frequencies larger than 400 Hz. The sampling duration was 10 s for each velocity component. This resulted in a time series of 10,000 measurements for each component. Although one flask rotation took about 0.4 s at 150 rpm and 0.3 s at 200 rpm, the long measurement duration (10 s) was intended to increase the reliability of the experiments by having enough replicates: 25 replicates at 150 rpm and 33 replicates at 200 rpm.

Results

The average radial and azimuthal water speeds, \bar{U} [Eq. (3)] are reported in Fig. 2 at select locations. The speed (i.e., magnitude of velocity) is used because it is not possible to ascertain the sense of the radial velocities. The sense of the azimuthal is known because the direction of rotation is known. The speeds values in Fig. 2 represent averages over 10 s at the reported locations.

Fig. 2 shows that the speeds in the SF increased with elevation

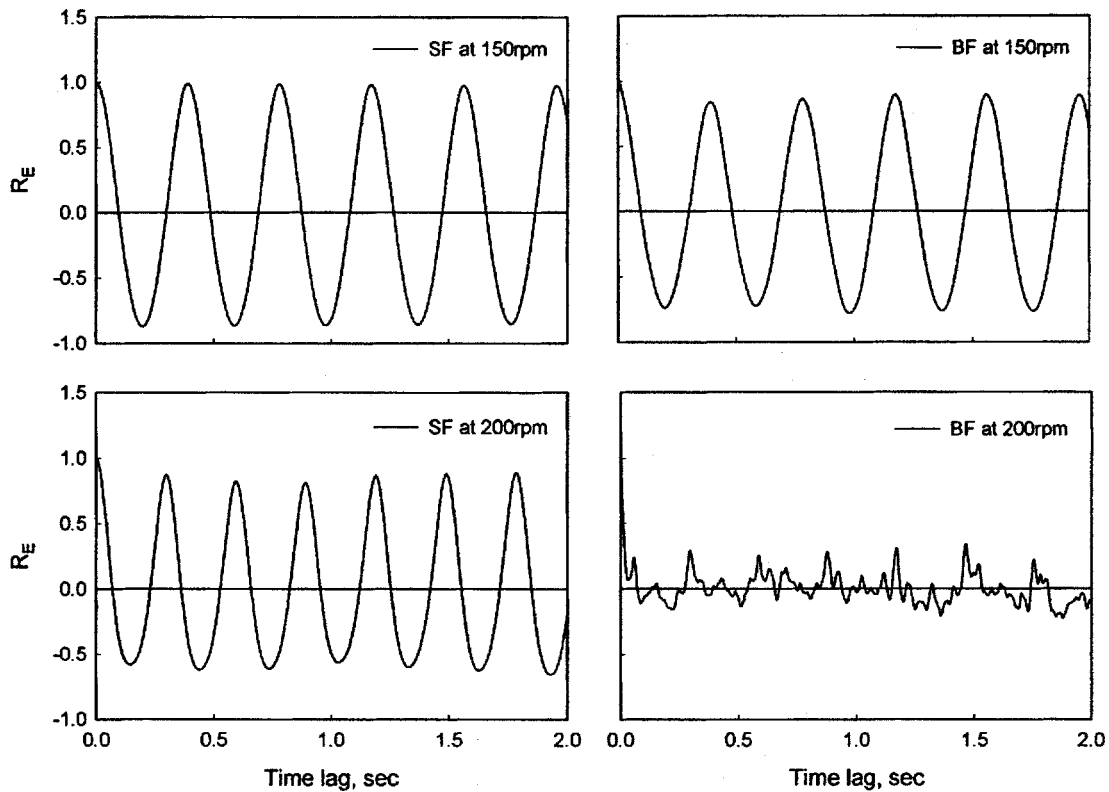


Fig. 3. Autocorrelation (azimuthal) plots at elevations of 3.6 cm in swirling flask and 1.4 cm in baffled flask. Integration of Eq. (7) occurs until first zero on time lag axis.

(i.e., when approaching the free surface) at both 150 and 200 rpm. There was a tendency for the azimuthal speed to increase with distance from the center, which is expected. The increase is clearest at 200 rpm. The radial water speed in the SF was practically independent of the distance from the center at 150 rpm, but displayed a slight increase with it at 200 rpm.

The speeds in the BF increased with elevation at 150 rpm, but the pattern reversed at 200 rpm. They tended to decrease outwards from the center at 150 rpm but increased at higher distances at 200 rpm. A large increase in the speed is noted in the center of the flask at 200 rpm at the highest elevation (2.4 cm).

At 150 rpm, the average of all speeds (azimuthal and radial) were 0.046 m/s in the SF and 0.27 m/s in the BF. At 200 rpm, they were 0.101 and 0.533 m/s for the SF and BF, respectively. Hence, the average speeds in both flasks almost doubled as the shaker rotation speed increased from 150 to 200 rpm.

The azimuthal speed in the SF at 200 rpm is very low in the core relative to the outer areas (Fig. 2). This is known as “solid body motion,” where shear flow (i.e., velocity gradient) is essentially absent (i.e., mixing is small). The speeds in the BF tended to be more variable in space displaying high and low values throughout the flask. In addition, while the speed in the SF decreased with depth, the speed profile in the BF displayed no discernible pattern, especially at 200 rpm. Note that the maximum speeds in the BF were about three times larger than the corresponding ones in the SF.

Fig. 3 shows plots of the autocorrelation function [Eq. (6)] as a function of the time lag τ between pairs of measurements. The periodic behavior of the motion is obvious in the SF at both RPMs and in the BF at 150 rpm; R_E takes alternating positive and negative values at lags coinciding with the rotation speed of the

flasks. Periodicity is also present in the BF at 200 rpm, though it is weaker.

To further investigate the effects of turbulence, in Figs. 4 and 5 we plotted the natural logarithm of the Fourier spectrum as function of the natural logarithm of frequencies of eddies for the azimuthal velocity. The spectra were computed by averaging the spectral amplitudes at all locations corresponding to the same frequencies. Figs. 4 and 5 also show the theoretical $-5/3$ slope based on Kolmogorov theory [Eq. (10)]. The observed spectra

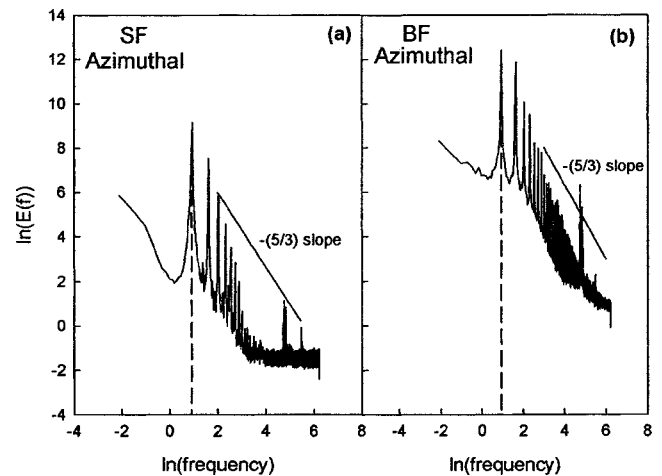


Fig. 4. Average one-dimensional energy spectra in swirling flask and baffled flask for 150 rpm based on azimuthal velocity. Peak on dashed line shows orbital shaker frequency of 2.5 Hz.

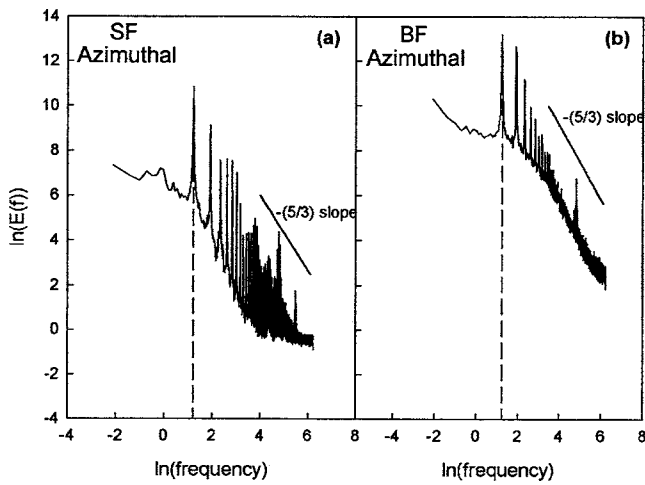


Fig. 5. Average one-dimensional energy spectra in swirling flask and baffled flask for 200 rpm based on azimuthal velocity. Peak on dashed line shows orbital shaker frequency of 3.33 Hz.

displayed periodicity, which is to be expected due to the periodic nature of the motion. The highest peak occurred at the frequency of rotation (150 or 200 rpm). The peaks that followed occurred at multiple frequencies of the main one. The spectra of radial speeds were similar and are not reported for brevity. The similarity indicated that the assumption of isotropic turbulence was valid. The peaks of the spectra in the BF were higher than that in the SF, indicating higher kinetic energy in the BF system. Also, the peaks of the spectra at 200 rpm were higher than those at 150 rpm, which indicates that there is an increase in energy dissipation of the system with the increase in orbital mixing speed.

For all spectra, one could stipulate the existence of a scaling regime (straight line behavior) that has periodicity superimposed on it. The periodicity is due to the large-scale flow (i.e., the flask motion), and it could be removed from the velocity field only if an analytical solution for the average velocity \bar{u} is available, as done in the work of Kitaigorodskii et al. (1983) while evaluating turbulence behavior below waves.

The flattening of the spectra at high frequencies is due to dominance of noise, especially at 150 rpm. But as the rpm increased to 200, the range of scaling appears to reach frequencies that were dominated by noise at 150 rpm. In other words, the smallest eddies at 200 rpm are smaller than the smallest eddies at 150 rpm. The spectra of the BF at 200 rpm provide clear evidence that the flow is turbulent, as the spectral slope approaches the $-5/3$ slope behavior.

The integral time scale [Eq. (5)] was numerically evaluated using Simpson's method (Kreyszig 1999; Press et al. 1992) by integrating from time zero to the time of the first zero crossing of the autocorrelation function. Data series at each location were smoothed, and these smoothed data were subtracted from the actual data to obtain turbulence data of 10,000 data points. The root mean square (RMS) value of the data series was obtained by squaring these turbulence values, then averaging them, and finally computing the square root of this average value.

Tables 1 and 2 report the flask-averaged root-mean-square values along with the flask-averaged integral time scale. The energy dissipation rate, ε , was estimated using Eq. (4) with the coefficient "A" set equal to 1.0. One value of ε , in azimuthal and radial direction, was computed at each location. The average of these two values was then obtained, and it is considered as representative of the energy dissipation at that location. Figs. 6 and 7 show these values in the SF and the BF, respectively, for two rotation speeds. The decimal logarithm was used for ease of visual interpretation of Figs. 6 and 7. The values of ε in the SF were higher at the surface and decreased rapidly with the increase in depth. The values of ε in the BF were much higher at the edges due to the presence of baffles. The flask-averaged value of ε , $\bar{\varepsilon}$, is reported in Tables 1 and 2.

The velocity gradient G was computed from Eq. (8) at each location using the local ε value for each velocity component. The local G value was obtained as the average of the two radial and azimuthal values. The flask-averaged velocity gradient, \bar{G} , is reported in Tables 1 and 2. Also reported is the value of G that corresponds to $\bar{\varepsilon}$, denoted by $G_{\bar{\varepsilon}}$. The Kolmogorov scale η was computed using water viscosity that corresponds to a water temperature of 20°C. The local η value was obtained as the average of the two values. The flask-averaged Kolmogorov scale, $\bar{\eta}$, was obtained by taking the arithmetic average of the local η values. The values are reported in Tables 1 and 2.

Discussion

The speeds in the BF were on the average five times larger than those in the SF for the corresponding rotation speed. This might be surprising considering that the two flasks contained the same water volume. However, we believe that two nonexclusive reasons caused the difference. First, the radius of the BF is 2.2 cm which is larger than the SF's radius of 1 cm. Hence noting that the azimuthal velocity could be approximated by the quantity (radius) \times (rotation speed), one would expect the speeds in the BF to be, on the average, 2.2 times those in the SF. Second, the geometry of

Table 1. Average Parameters for Flasks at 150 rpm

Type of flask	Mean velocity u_{avg} (m/s)	Root mean square velocity u'_{rms} (m/s)	Integral time scale τ_E (s)	Dissipation rate $\bar{\varepsilon}$ (m^2/s^3)	Average velocity gradient \bar{G} (s^{-1})	Kolmogorov microscale $\bar{\eta}$ (μm)	Velocity gradient of $\bar{\varepsilon}G_{\bar{\varepsilon}}$ (s^{-1})
Swirling Flask	0.0466	2.25×10^{-3}	0.073	(6.5×10^{-6}) 4.43×10^{-4} (2.0×10^{-3})	11.56	409.11	21.04
Baffled Flask	0.272	1.62×10^{-2}	0.0332	(1.9×10^{-3}) 1.55×10^{-2} (1.1×10^{-1})	96.97	115.66	124.49

Note: Values between parentheses represent minima and maxima of ε .

Table 2. Average Parameters for Flasks at 200 rpm

Type of flask	Mean velocity u_{avg} (m/s)	Root mean square velocity u'_{rms} (m/s)	Integral time scale τ_E (s)	Dissipation rate $\bar{\epsilon}$ (m^2/s^3)	Average velocity gradient \bar{G} (s^{-1})	Kolmogorov microscale $\bar{\eta}$ (μm)	Velocity gradient of $\bar{\epsilon}G_{\bar{\epsilon}}$ (s^{-1})
Swirling Flask	0.1013	5.41×10^{-3}	0.062	(1.9×10^{-5}) 2.07×10^{-3} (7.5×10^{-2})	28.84	245.28	45.49
Baffled Flask	0.533	4.95×10^{-2}	0.0218	(2.3×10^{-2}) 1.63×10^{-1} (1.0)	349.86	57.90	403.73

Note: Values between parentheses represent minima and maxima of ϵ .

the BF engendered high vertical velocities (observed visually). Based on the conservation of water mass [Eq. (11)], high vertical differential velocities result in high horizontal differential velocities. This could be simply noted if the spatial increments are made equal to each other, which indicates then that if the variation of u_z is large in the vertical direction, it would engender high velocity changes in the horizontal direction

$$\frac{\partial}{\partial x}(u_x) + \frac{\partial}{\partial y}(u_y) + \frac{\partial}{\partial z}(u_z) = 0 \quad (11)$$

The value of the Kolmogorov scale, $\bar{\eta}$, represents the size of the smallest eddies. If the smallest eddies are larger than the oil droplets, they tend to entrain oil droplets within them without breaking them. However, if the smallest eddies are smaller than an oil droplet, they would “share” it between them causing it to break. The size distribution of dispersed oil at sea was observed to range from 50 to about 500 μm (Delvigne 1983; Delvigne 1984; Byford and Green 1984; Mackay et al. 1986; Delvigne et al. 1987). The value of $\bar{\eta}$ in the SF at 150 rpm is about 410 μm . This implies that the mixing in the SF at 150 rpm does not theoretically create a high number of oil droplets whose sizes are smaller than 410 μm . This discrepancy indicates that there might be theoretical objections to using the mixing in the SF at 150 rpm to represent the mixing at sea. The average Kolmogorov scale in the BF at 200 rpm is about 50 μm , which should cause breakup of oil droplets approaching that scale.

Evidently, increasing the rotation speed of the SF would result in a decrease in the Kolmogorov scale, as noted in Tables 1 and 2. However, there are logistic limitations to increasing the speed. First, note that η is inversely proportional to ϵ to the power 1/4. Second, our own calculations showed that increasing the speed by 50 rpm resulted in a decrease in η to only 250 μm . Hence, the sought 50 μm in $\bar{\eta}$ might require a rotational speed of as high as 1,000 rpm.

Tables 1 and 2 report the flask-averaged velocity gradient, \bar{G} , along with $G_{\bar{\epsilon}}$ the velocity gradient corresponding to the flask-averaged energy dissipation rate, $\bar{\epsilon}$. The two quantities are significantly different. Some writers (Cleasby 1984; Clark 1985; Han and Lawler 1992) favor the use of one over another. We believe that the use of $\bar{\epsilon}$ is more physical due to the fact that ϵ represents an energy rate, while G represents a velocity gradient. Hence, $\bar{\epsilon}$ could be stipulated based on the law of conservation of energy. There is no counterpart for G (i.e., there is no law that requires the conservation of velocity or its gradient).

By accepting the conservation of ϵ as a necessary condition for replicating the mixing at sea, it is important to know the sea state corresponding to the values that we found in this study. Terray et al. (1996) conducted velocity measurements in the top 2

m of Lake Ontario and found ϵ to vary between 10^{-5} and $10^{-2} m^2/s^3$. The significant wave height in that study was about 0.25 m. Drennan et al. (1996) conducted similar measurements in the Atlantic Ocean off of the Maryland Coast. They found ϵ varying between 10^{-4} and $5.0 \times 10^{-4} m^2/s^3$. The significant wave height was about 1.0 m. These values are smaller than those reported by Terray et al. (1996) despite the fact that the wave height was four times larger. However, as discussed by Drennan et al. (1996), the measurements of Terray et al. (1996) were in strongly forced fetch-limited waves, whereas those of Drennan et al. (1996) represent fully developed sea with an almost infinite fetch (the Atlantic Ocean). Delvigne and Sweeney (1988, p. 6) reported that ϵ varies between 10^{-3} and $10^{-2} m^2/s^3$ for the surface layer and between 1 and $10 m^2/s^3$ for breaking waves. However, they do not define the “surface layer” nor did they explain the type of wave breaker. It appears therefore, that additional studies are needed to quantify and define ϵ at sea. But the flexibility in obtaining high values of ϵ in the BF makes using it preferable to using the SF.

The use of an average value of ϵ is probably more plausible for the BF than for the SF; when one uses a spatially averaged value, such as $\bar{\epsilon}$, as representative of the mixing regime, it is preferable that the spatial distribution does not follow a pattern. The mixing in the SF is greatest at the outer edge near the surface and decreases with depth and/or when approaching the center (see Figs. 2 and 6). In essence, there are several zones in the SF with different mixing characteristics. A spatial average might not have much physical significance in such a case. The velocities (and

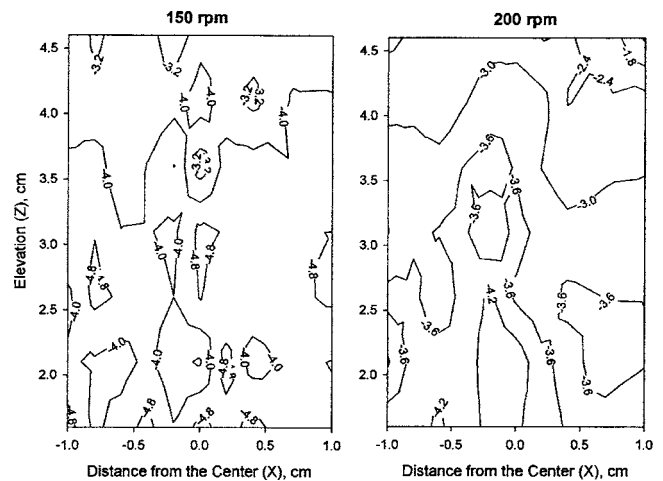


Fig. 6. Contour plots of $\log(\epsilon)$ in Erlenmeyer flask at 150 and 200 rpm. Label represents values of $\log(\epsilon)$.

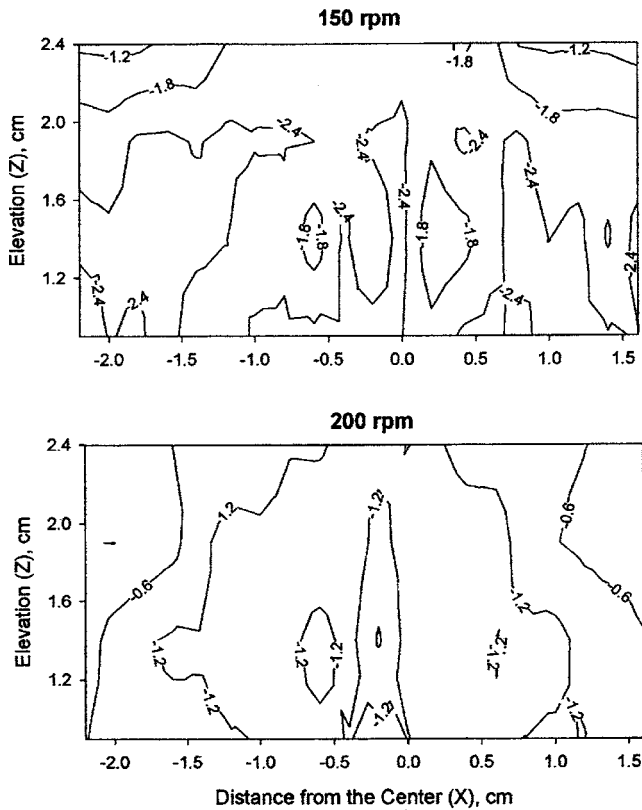


Fig. 7. Contour plots of $\log(\varepsilon)$ in baffled flask at 150 and 200 rpm. Label represents values of $\log(\varepsilon)$.

subsequently the local ε values) in the BF were distributed more evenly throughout the flask, such that a clear pattern did not exist (Figs. 2 and 7).

Conclusions

Two components of instantaneous velocity were used to characterize turbulent flow in the SF and the BF using an HWA. General flow patterns, turbulent flow parameters, and local dissipation rates were determined. The study shows that the mixing in the BF

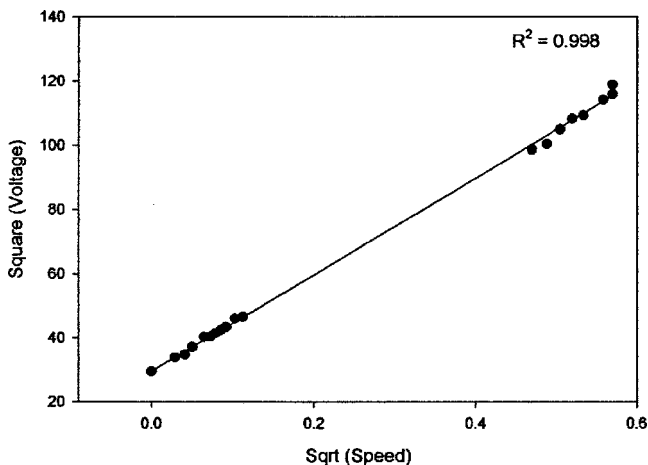


Fig. 8. Calibration curve of hot-wire anemometer

is more uniformly distributed than in the SF. The approximation of local isotropy was supported by $(-5/3)$ slope of the turbulence frequency spectra in case of the BF.

Flask average energy dissipation rates in the SF were about 2 orders of magnitude smaller than those in the BF. The sizes of the microscales in the BF were found to be much smaller than that in the SF. Also, in the BF, the sizes of the microscales approached the size of oil droplets observed at sea (50–400 μm) (Delvigne 1983; Byford and Green 1984; Mackay et al. 1986; Delvigne et al. 1987). This could be used to infer that the turbulence in the BF closely resembles the turbulence occurring in the top few centimeters of a breaking wave. Hence, the BF is preferable as a laboratory surrogate for dispersant testing.

Acknowledgment

This research was supported, in part, by the U.S. Environmental Protection Agency through Contract No. PR-OH-01-00381. However, no official endorsement of the results should be implied.

Appendix. Calibration of Hot-Wire Anemometer

The hot-wire probe was calibrated against the velocity values obtained by a pitot tube in a recirculating type water channel. The theory of cooling of hot wire is known as King's law (King 1914), which states that the square of HWA output voltage, E , varies linearly with the square root of the fluid's speed, u . The fit in Fig. 8 gave the constants, resulting in the equation

$$E^2 = 150.71\sqrt{u} + 29.497 \quad (12)$$

The high R^2 value of the fit along with visual observation of Fig. 8 indicate that the fit was excellent.

Notation

The following symbols are used in this paper:

- A = constant of order one;
- G = local velocity gradient (s^{-1});
- \bar{G} = flask average velocity gradient (s^{-1});
- $G_{\bar{\varepsilon}}$ = flask velocity gradient based on $\bar{\varepsilon}$ (s^{-1});
- L = integral length scale (m);
- N = orbital shaker speed (rpm);
- R_E = autocorrelation coefficient function;
- \bar{U}_i = time-averaged (mean) velocity;
- u_i = instantaneous velocity;
- u'_i = randomly fluctuating velocity;
- \bar{u}_i = regular oscillatory component of velocity;
- ε = local energy dissipation rate (m^2/s^3);
- $\bar{\varepsilon}$ = flask average energy dissipation rate (m^2/s^3);
- η = local Kolmogorov microscale (μm);
- $\bar{\eta}$ = flask average Kolmogorov scale (μm);
- ν = kinematic viscosity (m^2/s);
- τ = time lag (s); and
- τ_{E_i} = integral time scale (s).

References

- Anderson, D. A., Tannehill, J. C., and Pletcher, R. H. (1984). *Computational fluid mechanics and heat transfer*, Hemisphere, New York.
- Batchelor, G. K. (1970). *The theory of homogeneous turbulence*, The University Press, Cambridge, U.K.
- Byford, D. C., and Green, P. J. (1984). "A view of the Mackay and Labofina laboratory tests for assessing dispersant effectiveness with regard to performance at sea." *Oil spill chemical dispersants: Research, experience, and recommendations*, STP 840, T. E. Allen, ed., American Society of Testing and Materials, Philadelphia, 69–86.
- Camp, T. R., and Stein, P. C. (1943). "Velocity gradient and internal work in fluid motion." *J. Boston Soc. Civ. Eng.*, 30(4), 219–237.
- Canevari, G. P., Calcavecchio, P., Lessard, R. R., Becker, K. W., and Fiocco, R. J. (2001). "Key parameters affecting the dispersion of viscous oil." *Proc., 2001 Int. Oil Spill Conf.*, American Petroleum Institute, Washington, D.C., 479–483.
- Clark, M. M. (1985). "A critique of Camp and Stein's RMS velocity gradient." *J. Environ. Eng.*, 111(6), 741–754.
- Clayton, J. R., Payne, J. R., and Farlow, J. S. (1993). "EPA technical project monitor." *Oil spill dispersants, mechanical action, and laboratory tests*, CK Smoley, Boca Raton, Fla.
- Cleasby, J. L. (1984). "Is velocity gradient a valid turbulent flocculation parameter?" *J. Environ. Eng.*, 110(5), 875–897.
- Delvigne, G. A. L. (1983). "Sea measurements on natural and chemical dispersion of oil." *Rep. No. M1933-I*, Delft Hydraulics Laboratory, Delft, The Netherlands.
- Delvigne, G. A. L. (1984). "Laboratory facility for the simulation of the natural and chemical dispersion of oil." *Rep. No. M1933-II*, Delft Hydraulics Laboratory, Delft, The Netherlands.
- Delvigne, G. A. L. (1993). "Natural dispersion of oil by different sources of turbulence." *Proc., Int. Oil Spill Conf.*, American Petroleum Institute, Washington, D.C., 415–419.
- Delvigne, G. A. L., and Sweeney, C. E. (1988). "Natural dispersion of oil." *Oil Chemical Pollution*, 4, 281–310.
- Delvigne, G. A. L., van der Stel, J. A., and Sweeney, C. E. (1987). "Measurement of vertical turbulent dispersion and diffusion of oil droplets and oiled particles." *Rep. No. Z75-2*, Delft Hydraulics Laboratory, Delft, The Netherlands.
- Drennan, W. M., Donelan, M. A., Terray, E. A., and Katsaros, K. B. (1996). "Oceanic turbulence dissipation measurements in SWADE." *J. Phys. Oceanogr.*, 26, 808–815.
- Fingas, M. F. (1991). "Dispersants: A review of effectiveness measures and laboratory physical studies." *Proc., Alaska RRT Dispersant Workshop*, U.S. Minerals Management Service, Anchorage, Alaska.
- Fingas, M. F. (2000). "Use of surfactants for environmental applications." *Surfactants: Fundamentals and applications to the petroleum industry*, L. Laurier Schramm, ed., Chap. 12, Cambridge Univ. Press, Cambridge, U.K., 461–539.
- Fingas, M. F., Bier, I., Bobra, M., and Callaghan, S. (1991). "Studies on the physical and chemical behavior of oil and dispersant mixtures." *Proc., 1991 Int. Oil Spill Conf.*, American Petroleum Institute, Washington, D.C., 411–414.
- Fingas, M. F., Bobra, M. A., and Velicogna, R. K. (1987a). "Laboratory studies of the chemical and natural dispersibility of oil." *Proc., Int. Oil Spill Conf.*, American Petroleum Institute, Washington, D.C., 241–246.
- Fingas, M. F., Huang, E., Fieldhouse, B., Wang, L., and Mullin, J. V. (1997). "The effect of energy, settling time and shaking time on the swirling flask dispersant apparatus." *Proc., 20th Arctic Marine Oil Spill Program Technical Seminar*, Environment Canada, Ottawa, 541–550.
- Fingas, M. F., Hughes, K. A., and Schweitzer, M. A. (1987b). "Dispersant testing at the Environmental Emergencies Technology Division." *Proc., 10th Arctic Marine Oil Spill Program Technical Seminar*, Conservation and Protection, Edmonton, Canada, 343–356.
- Fiocco, R. J., Daling, P. S., DeMarco, G., Lessard, R. R., and Canevari, G. P. (1999). "Chemical dispersibility study of heavy bunker fuel oil." *Proc., 22nd Arctic Marine Oil Spill Program Technical Seminar*, Environment Canada, Ottawa, 173–186.
- Frost, W. (1977). "Spectral theory of turbulence." *Handbook of turbulence*, W. Frost and T. M. Moulden, Editors, Vol. I, Plenum, New York, 85–125.
- Han, M., and Lawler, D. F. (1992). "The (relative) insignificance of G in flocculation." *J. Am. Water Works Assoc.*, 84(10), 79–91.
- Hinze, J. O. (1987). *Turbulence, An introduction to its mechanisms and theory*, 2nd Ed., McGraw-Hill, New York.
- Kaku, V. J., Boufadel, M. C., and Venosa, A. D. (2002). "Evaluation of mixing energy in the swirling and baffled flasks." *Proc., Oil Spill Conf.*, Wessex Institute of Technology, Rhodes, Greece, 211–218.
- King, L. V. (1914). "On the convection of heat from small cylinders in a stream of fluid: Determination of the convection constants of small platinum wires with applications to hot-wire anemometry." *Philos. Trans. R. Soc. London, Ser. A*, A214, 373–432.
- Kitaigorodskii, S. A., Donelan, M. A., Lumley, J. L., and Terray, E. A. (1983). "Wave-turbulence interactions in the upper ocean. Part II: Statistical characteristics of wave and turbulent components of the random velocity field in the marine surface layer." *J. Phys. Oceanogr.*, 13, 1988–1999.
- Kolmogorov, A. N. (1941). "The local structure of turbulence in incompressible viscous fluid for very large Reynolds number." *Dokl. Akad. Nauk SSSR*, 30, 9–13.
- Kolmogorov, A. N. (1962). "A refinement of previous hypotheses concerning the local structure of turbulence in a viscous incompressible fluid at high Reynolds number." *J. Fluid Mech.*, 13, 82–85.
- Kresta, S. M., and Wood, P. E. (1993). "The flow field produced by a pitched blade turbine: Characterization of the turbulence and estimation of the dissipation rate." *Chem. Eng. Sci.*, 48(10), 1761–1774.
- Kreyszig, E. (1999). *Advanced engineering mathematics*, 8th Ed., Wiley, New York.
- Lunel, T. (1993). "Dispersion: Oil drop size measurements at sea." *Proc., 16th Arctic and Marine Oil Spill Program*, Environment Canada, Calgary, Canada, 1023–1057.
- Lunel, T., and Davies, L. (1996). "Dispersant effectiveness in the field on fresh oils and emulsions." *Proc., 1996 Arctic and Marine Oil Spill Programme (AMOP)*, Environment Canada, Ottawa, Canada, 1355–1394.
- Mackay, D., Chau, A., and Poon, Y. C. (1986). "A study of the mechanism of chemical dispersion of oil spills." *Publication EE-76*, Environmental Protection Agency, Ottawa, 150.
- Martinelli, F. N. (1984). "The status of Warren Spring Laboratory's rolling flask test." *Oil spill chemical dispersants, Research experience and recommendations*, ASTM 840, T. E. Allen, ed., American Society of Testing and Materials, Philadelphia, 55–68.
- Monin, A. S., and Yaglom, A. M. (1975). *Statistical fluid mechanics: Mechanics of turbulence*, Vol. 2, MIT Press, Cambridge, Mass.
- Naess, A. (1979). "Mixing of oil spills into the sea by breaking waves." *Proc., 11th Annual Offshore Technical Conf.*, Houston, 2193.
- National Research Council (NRC). (1989). *Using oil spill dispersants on the sea*, National Academy Press, Washington, D.C.
- Nordvik, A., Hudon, T., and Osborn, H. (1993). "Interlaboratory calibration testing of dispersant effectiveness." *Marine Spill Response Corporation Technical Rep., Series 93-003*, Washington, D.C.
- Patterson, G. K., and Zipp, R. P. (1991). "Turbulence and mixing: Modeling effects on chemical reactions." *Mixing in coagulation and flocculation*, A. Amirthrajah, M. M. Clark, and R. R. Trussel, eds., American Water Works Research Foundation, Denver.
- Press, W. H., Teukolsky, S. A., Vetterling, W. T., and Flannery, B. P. (1992). *Numerical recipes in Fortran 77: The art of scientific computing*, 2nd Ed., Cambridge Univ. Press, New York.
- Rao, M. A., and Brodkey, R. S. (1972). "Continuous flow stirred tank turbulence parameters in the impeller stream." *Chem. Eng. Sci.*, 27, 137–156.
- Tennekes, H., and Lumley, J. L. (1972). *A first course in turbulence*, MIT

Press, Cambridge, Mass., 300.

- Terray, E. A., Donelan, M. A., Agrawal, Y. C., Drennan, W. M., Kahma, K. K., Williams, A. J., III, Hwang, P. A., and Kitaigorodskii, S. A. (1996). "Estimates of kinetic energy dissipation under breaking waves." *J. Phys. Oceanogr.*, 26, 792–807.
- Venosa, A. D., King, D. W., and Sorial, G. A. (2002). "The baffled flask test for dispersant effectiveness: A round robin evaluation of reproducibility and repeatability." *Spill Sci. Technol. Bulletin*, 7(5),

299–308.

- Wu, H., and Patterson, G. K. (1989). "Laser doppler measurements of turbulent flow parameters in a stirred mixer." *Chem. Eng. Sci.*, 44, 2207–2221.
- Wu, H., Patterson, G. K., and van Doorn, M. (1989). "Distribution of turbulence energy dissipation rates in a Rushton turbine stirred mixer." *Exp. Fluids*, 8, 153–160.